On molar- and mass-based approaches to single component drop evaporation modelling

S. Tonini, G.E. Cossali

Department of Engineering and Applied Sciences, University of Bergamo,

Viale Marconi 5, 24044 Dalmine, Italy

June 11, 2016

Abstract

Different approaches to model evaporation from single-component spherical liquid drop floating in a gaseous environment are analysed. The species conservation equations in molar and mass form are solved to yield different drop evaporation models. Two of them rely on the widely used assumption of constant (molar or mass) density and yield an explicit formula for the evaporation rate, whereas the third model relieves the constant density hypothesis and yields the evaporation rate in implicit form. The comparison among the results predicted by the models is made for a relative wide range of temperature, pressure and Reynolds number operating conditions and for different liquids, like water, alcohols, ketones and hydrocarbons.

1 Nomenclature

A	Coefficient (equation 27)	-
B_M, B_M^*	Spalding and modified Spalding mass transfer number	-
c	molar density	$kmol\ m^{-3}$
c_p	specific heat	$J\ kg^{-1}K^{-1}$
D_{pk}	binary diffusion coefficient	m^2s^{-1}
$F(-)$	function (equation 23)	-
k	thermal conductivity	$W\ m^{-1}K^{-1}$
Le	modified Lewis number, $= \frac{k}{cMmD_{10}c_p}$	-
m_{ev}	evaporation rate	$kg\ s^{-1}$
Mm	molar mass	$kg\ kmol^{-1}$
n_r	mass flux radial component	$kg\ m^{-2}s^{-1}$
$\mathbf{n}$	mass flux	$kg\ m^{-2}s^{-1}$
$\mathbf{N}$	molar flux	$kmol\ m^{-2}s^{-1}$
P_T	total pressure	Pa
$P_{v,s}$	saturation vapour pressure	Pa
$\dot{Q}$	heat flux	W
r	radial coordinate	m
$\bar{R}$	universal gas constant	$J\ kmol^{-1}K^{-1}$
Re	Reynolds number, $= \frac{2\rho Vel\ R_0}{\nu}$	-
R_0	drop radius	m
Sc	Schmidt number, $= \frac{\nu_{ref}}{D_{10}\rho}$	-
Sh_0	Sherwood number, $= 2 + 0.552\,\mathrm{Re}^{1/2}\,Sc^{1/3}$	-
Sh	modified Sherwood number (equation 23)	-
T	temperature	K
$\tilde{T}$	non-dimensional temperature	-
U	Stefan velocity	$m\ s^{-1}$
Vel	drop/gas relative velocity	$m\ s^{-1}$
y	molar fraction	-
Y	non-dimensional evaporation rate	-

Greek symbols

ζ non-dimensional radial coordinate $\left(\zeta = \frac{R_0}{r}\right)$ -

θ non-dimensional molar mass ratio $\left(\theta = \frac{Mm^{(1)} - Mm^{(0)}}{Mm^{(0)}}\right)$ -

Λ non-dimensional parameter (equation 14)   -

ρ mass density $kg\ m^{-3}$

ν viscosity $kg\ m^{-1}s^{-1}$

χ mass fraction   -

Subscripts

0   gas

1   vaporising species

ref reference

s drop surface

v vapour

∞ ambient conditions

Superscripts

mas mass

mol molar

T total

2   Introduction

The modelling of liquid drop evaporation in gaseous environment has been the topic of extensive research since the nineteenth century, when Maxwell [1] proposed the first model on this subject. Since then the interest on this phenomenon has grown, driven by its importance in a wide range of applicative fields, like spray combustion, spray painting, fire control, medical applications, etc. [2].

The evaporation process can be treated using the analogy between heat and mass transfer only for weak evaporation conditions (i.e. low mass transfer rates) [3], whereas in case of high mass transfer rates, like for a drop evaporating in a high temperature gas, mass and heat transfer processes should be considered distinctly, but accounting for the

coupling produced by the presence of the Stefan flow [4].

Despite the wide scientific literature available on this topic (refer to [6] and [7] for recent thorough reviews), different aspects still remain unknown. Furthermore, to numerically simulate the evaporation in multi-particle systems (like sprays or aerosols) using CFD methodologies, detailed models able to catch the complexity of the phenomenon have to be simplified to be CPU efficient, leading to the introduction of many simplifying approximations like quasi-steadiness, drop sphericity, constant physical properties within the gas and liquid phases, uniform drop temperature and composition, to cite the most common ones. Referring to this category of evaporation models, the most widespread one, which is nowadays implemented in most of commercial and in-house CFD codes for dispersed flow modelling, is likely that proposed by Abramzon and Sirignano back in 1989 [8].

Extensive research was carried on over the years (see [7] for reference) to investigate the mass and thermal phenomena occurring within the liquid phase and various models became available in the literature. Improvements of the first simplified model, which assumes uniform liquid temperature and composition [9], [10], were obtained by considering temperature and/or concentration gradients within the liquid phase, introducing a finite conductivity/diffusivity [11], [12].These models were successively refined by introducing an effective conductivity/diffusivity to account for the effect on inner recirculation [8]. Unsteadiness of the evaporation phenomenon, accounting for moving boundary effect due to drop shrinking, was recently addressed by [13], [14], confirming that this phenomenon cannot be neglected when detailed predictions are required.

The complex physical and computational aspects related to the modelling of drop evaporation, like liquid composition, drop shape, detailed evaluation of thermophysical properties, interaction with other substrates (either liquid or solids), etc., have been addressed over the last decades mainly by refined numerical models (refer to [15], [16], [17], [18], [19] for pioneering and recent works on the numerical modelling of single liquid drop evaporating in gaseous environment). The results from these studies allowed to deepen the knowledge of this complex phenomenon, owing to the possibility of analysing details otherwise difficult to evaluate, and they can be practically used as benchmarking for the development of simplified models for spray applications that, as pointed out above, must necessarily require a much lower computational effort.

The classical approach to model the vapour transport through the gas phases relies on the constancy of the gas density, which cannot obviously represent correctly the physics of the phenomenon when the gas and the drop

temperature differ noticeably. Recently a model relieving such hypothesis was proposed in [20] and [21], but since the evaporation rate is evaluated in implicit form, this model is computationally less efficient when implemented in a CFD code; models relaying on the constancy of gas density are then still preferred for multi-particle applications.

Constitutive equations are an important issue for evaporation modelling and, for single component drop evaporation, the widely accepted Stefan-Maxwell equations can be reduced to the well-known Fick's law, that can be expressed equivalently in molar or in mass form [22]. Simplified solutions can be obtained from both forms, but different approximations must be imposed, yielding different solutions. The mass based form of the mentioned equations has been largely used to develop the previously mentioned simplified models (see [4], [8]) imposing the constancy of gas density and obtaining a simple explicit relation for evaluating the evaporation rate. The molar based form of such equations, that, as previously mentioned, is perfectly equivalent to the mass form, can also be used, but a simple solution can only be found by imposing the constancy of the molar density, and due to this different assumption the solution is different from the classical one.

The aim of the present work is to quantitatively investigate the role of each of the two approximations in order to evidence the effect on the quantitative prediction of the evaporation rate from a spherical drop floating in a gaseous environment. The description of the mathematical models and the derivation of the analytical solutions are briefly summarised in the following section, followed by a discussion on the comparison among the model results.

3   Model equations

The equations needed to model the steady evaporation from a drop in a gaseous environment are reported in the following sections. Molar and mass forms of the conservation and constitutive equations are solved under three different assumptions on the gaseous mixture density, yielding three different evaporation models.

3.1   Species conservation and constitutive equations

The diffusion of multicomponent species in a mixture can be modelled by the Stefan-Maxwell equations [22] and a simplified form for a mixture of $n + 1$ species, neglecting Soret effect and diffusion due to pressure gradients and to

external force, is [22]:

$$\boldsymbol{\nabla} y^{(p)} = \sum_{k=0}^{n} \frac{1}{cD_{pk}} \left(y^{(p)} \mathbf{N}^{(k)} - y^{(k)} \mathbf{N}^{(p)} \right) \tag{1}$$

where $y^{(p)}$ is the molar fraction of the p-component, $\mathbf{N}^{(p)}$ is the molar flux of the p-component, c is the molar density and $D_{pk} = D_{kp}$ is the binary diffusion coefficient of p-component into k-component. The evaporation of a multicomponent drop can then be modelled on the basis of equations (1) and an exact solution for multicomponent spherical drops is given in [23].

When the evaporation of a single component drop is considered, the above constitutive equations can be simplified to:

$$\mathbf{N}^{(p)} = y^{(p)} \mathbf{N}^{(T)} - cD_{10} \boldsymbol{\nabla} y^{(p)}; \qquad p = 0,1 \tag{2}$$

where $\mathbf{N}^{(T)} = \mathbf{N}^{(0)} + \mathbf{N}^{(1)}$ and hereinafter the index 0 will always refer to the species that is not part of the liquid drop composition.

Equations (2) are a way to state the Fick's law of diffusion [22] and it should be noticed that the two equations are linearly dependent. Equations (2) can also be written in term of mass fluxes $\mathbf{n}^{(p)}$, that are related to the molar fluxes by $\mathbf{n}^{(p)} = \mathbf{N}^{(p)} Mm^{(p)}$ where $Mm^{(p)}$ is the p-component molar mass:

$$\mathbf{n}^{(p)} = \chi^{(p)} \mathbf{n}^{(T)} - \rho D_{10} \boldsymbol{\nabla} \chi^{(p)}; \quad p = (0,1) \tag{3}$$

where ρ is the mixture mass density and $\chi^{(p)}$ is the mass fraction of the p-species, which is related to the molar fraction according to:

$$y^{(p)} = \frac{\rho}{cMm^{(p)}} \chi^{(p)} \tag{4}$$

To notice that equations (3), that for single-component drop ($n = 1$ in equations 1) are equivalent to equations (2) since they are both a direct consequence of equations (1), are often used to model also multi-component drop evaporation (see for example [24], [25], [26]), but in such case they must be considered an approximation of (1), valid for dilute mixtures, and the two forms (molar (2) and mass (3)) are not equivalent.

When modelling steady drop evaporation, the liquid-gas interface is often assumed to be still and the diffusion of the gas species through the liquid is considered to be negligible; this implies that the gas ($p = 0$) flux is nil everywhere i.e. $\mathbf{n}^{(0)} = Mm^{(0)} \mathbf{N}^{(0)} = 0$.

Equations (2) and (3) can then be written for the gas species as:

$$\mathbf{N}^{(T)} = cD_{10}\boldsymbol{\nabla}\ln y^{(0)}; \quad \mathbf{n}^{(T)} = \rho D_{10}\boldsymbol{\nabla}\ln\chi^{(0)} \tag{5}$$

and the equations for $p = 1$ can be disregarded since they are redundant.

The steady-state species conservation equations for both molar and mass cases are given by [22]:

$$\nabla \cdot \mathbf{N}^{(p)} = 0; \quad \nabla \cdot \mathbf{n}^{(p)} = 0$$

and summation over the index p yields the usual mass conservation equation:

$$\nabla \cdot \mathbf{N}^{(T)} = 0; \quad \nabla \cdot \mathbf{n}^{(T)} = 0 \tag{6}$$

To noticed that for the spherical drop case the only non-nil component of the fluxes is the radial one and that the mass averaged velocity (Stefan velocity) can be defined from the equation: $\rho U = n_r^{(T)}$ and consequently the mass conservation equation can be written as:

$$\frac{\partial r^2 \rho U}{\partial r} = 0 \tag{7}$$

3.2 The temperature field

The mixture density, that hereinafter will be considered an ideal mixture of perfect gases, depends on the temperature field, which can be found solving the energy equation for steady-state conditions in radial symmetry, neglecting minor terms like dissipation from viscous stresses, species excess kinetic energy, and work of pressure forces (see [22] for the complete equation):

$$\rho U c_p \nabla_r T - k\nabla^2 T = 0$$

Since the solution of equation (7) yields:

$$\rho U = \frac{m_{ev}}{4\pi r^2} \tag{8}$$

where m_{ev} is the evaporation rate ($n^{(0)}$ is nil everywhere), imposing the first kind B.C., $T(R_0) = T_s$; $T(\infty) = T_\infty$, yields the following temperature field:

$$\tilde{T} = \frac{1 - \tilde{T}_s}{1 - e^{-Y}} + \frac{\tilde{T}_s - e^{-Y}}{1 - e^{-Y}}e^{-Y\zeta} \tag{9}$$

where $\tilde{T} = \frac{T}{T_\infty}$, $\zeta = \frac{R_0}{r}$ and $Y = \frac{m_{ev}c_{p,ref}}{4\pi R_0 k_{ref}}$ is a non-dimensional form of the evaporation rate. The values of the specific heat (c_{ref}) and thermal conductivity (k_{ref}) are evaluated at a reference conditions, for example through the "1/3-law" proposed by [27]. The heat flux can then be evaluated as:

$$\dot{Q} = 4\pi R_0 k_{ref} \left(T_\infty - T_s \right) \frac{Y}{e^Y - 1} \tag{10}$$

3.3   Evaporation models

Equations (2) or (3) can be solved to yield the vapour concentration distribution and the vapour flux at the drop surface, from which the evaporation rate can be easily calculated. In doing so, different assumptions can be made. The classical single component drop evaporation model (see for example [4]) is obtained by integrating the second of equations (5) in spherical coordinates, allowing for equation (8) with the further assumption of a constant mass density ρ_{ref} , usually evaluated at a reference condition through the already mentioned "1/3-law". Imposing the boundary conditions:

$$\chi^{(0)} \left(R_0 \right) = \chi_s^{(0)}; \quad \chi^{(0)} \left(\infty \right) = \chi_\infty^{(0)}$$

yields the solution:

$$\ln \chi^{(0)} = \left(\ln \frac{\chi_s^{(0)}}{\chi_\infty^{(0)}} \right) \frac{R_0}{r} + \ln \chi_\infty^{(0)}$$

and then the non-dimensional form of the evaporation rate Y^{mas}:

$$Y^{mas} = \frac{m_{ev}^{mas} c_{p,ref}}{4\pi R_0 k_{ref}} = \frac{\rho_{ref}}{c_{ref} M m^{(1)}} \frac{1}{Le} \ln \left(\frac{1 - \chi_\infty^{(1)}}{1 - \chi_s^{(1)}} \right) \tag{11}$$

where $Le = \frac{k_{ref}}{c_{ref} M m^{(1)} D_{10,ref} c_{p,ref}}$ is a modified Lewis number. It should be stressed that the numerical value of Le is only slightly dependent on the reference temperature since the temperature dependence of k_{ref}, c_{ref} and $D_{10,ref}$ practically cancels out in the definition of Le.

Equation (11), that holds for a drop evaporating in a stagnant gas (i.e. $Re = 0$), is the basis of the already mentioned model of Abramzon and Sirignano [8], that extends the result to large Re and will be reported in the next section.

Integrating the second of equations (5) in spherical coordinates, assuming a constant molar density c_{ref} (again evaluated at reference conditions) yields, in a way similar to that described above, the following result for the

non-dimensional evaporation rate:

$$Y^{mol} = \frac{m_{ev}^{mol} c_{p,ref}}{4\pi R_0 k_{ref}} = \frac{1}{Le} \ln \left(\frac{1 - y_\infty^{(1)}}{1 - y_s^{(1)}} \right) \tag{12}$$

It is important to notice that, although the equations (2) and (3) are equivalent, the integrations above described are based on different assumptions (constancy of mass density for equation (3) and of molar density for equation (2)) and the resulting solutions are then different, since generally:

$$Mm^{(1)} c_{ref} \ln \left(\frac{1 - y_\infty^{(1)}}{1 - y_s^{(1)}} \right) \neq \rho_{ref} \ln \left(\frac{1 - \chi_\infty^{(1)}}{1 - \chi_s^{(1)}} \right) \tag{13}$$

apart of the special case when $\theta = \frac{Mm^{(1)} - Mm^{(0)}}{Mm^{(0)}} = 0$ (i.e. when $Mm^{(1)} = Mm^{(0)}$, like for example for a methanol drop evaporating in oxygen), in fact in such case: $y^{(p)} = \chi^{(p)}$ and $\frac{\rho_{ref}}{c_{ref} Mm^{(1)}} = 1$.

Since the second approach is as justified as the first one, it is worth to investigate which of them is the most accurate, if any. To this end the results of the two approaches can be compared with those obtained solving the conservation equations (2 or 3) without assuming a constant molar or mass density, in such case both solutions are identical. This approach is reported in [20] and consists in considering also the momentum equation among the balance equation set, and showing that for:

$$\Lambda = \frac{\bar{R} T_\infty R_0^2}{Mm_v D_{10,ref}^2} \to \infty \tag{14}$$

which is a quite acceptable assumption for practical applications, the combination of momentum, energy and species conservation yields the constancy of the pressure across all the gas phase:

$$P_{T,\infty} = \left(1 + \theta \chi^{(0)} \right) \rho \frac{\bar{R} T}{Mm_v} = c \bar{R} T = const \tag{15}$$

The solution reported in [20] was derived using the mass form of equations (5) yielding the following implicit equation for the non-dimensional evaporation rate:

$$Y + \left(\tilde{T}_s - 1 \right) \left(\frac{Y}{1 - e^{-Y}} - 1 \right) = \frac{1}{Le} \ln \left[\frac{\left(1 - \theta \chi_\infty^{(0)} \right) - \frac{P_{v,s} Mm^{(1)}}{\bar{R} T_\infty \rho_\infty}}{(1 + \theta) \left(1 - \chi_\infty^{(1)} \right)} \right] \tag{16}$$

A simpler form can be obtained transforming equation (16) using equation (4) and the relation:

$$y_s^{(1)} = \frac{P_{v,s}}{P_T} \tag{17}$$

9

or directly solving the first of equations (5) with the same method used in [20], yielding:

$$Y = \frac{c_\infty}{c_{ref} \int_0^1 \tilde{T}(\zeta)\, d\zeta} \frac{1}{Le} \ln \frac{1 - y_\infty^{(1)}}{1 - y_s^{(1)}} \tag{18}$$

with

$$\int_0^1 \tilde{T}\, d\zeta = \frac{\tilde{T}_s - e^{-Y}}{1 - e^{-Y}} + \frac{1 - \tilde{T}_s}{Y} \tag{19}$$

As reported in [21], also this model, that holds for $Re = 0$, can be extended to include the effect of convective flow, as it will be described in the next section.

3.4 Extension to convective conditions ($Re > 0$)

The above reported models can be extended to convective conditions ($Re > 0$) by the film theory approach, as reported in [8] and [21]. The non-dimensional evaporation rates can thus be written as:

$$Y^{mas} = \frac{Sh(B_M)}{2} \frac{\rho_{ref}}{c_{ref} Mm^{(1)}} \frac{1}{Le} \ln(1 + B_M) \tag{20}$$

$$Y^{mol} = \frac{Sh(B_M^*)}{2} \frac{1}{Le} \ln(1 + B_M^*) \tag{21}$$

$$Y = \frac{Sh(B_M^*)}{2} \frac{c_\infty}{c_{ref} \int_0^1 \tilde{T}(\zeta)\, d\zeta} \frac{1}{Le} \ln(1 + B_M^*) \tag{22}$$

where $B_M = \frac{\chi_s^{(1)} - \chi_\infty^{(1)}}{1 - \chi_s^{(1)}}$ is the Spalding mass transfer number [8], $B_M^* = \frac{y_s^{(1)} - y_\infty^{(1)}}{1 - y_s^{(1)}}$ is the modified Spalding mass transfer number [20], Sh is a modified Sherwood number that is calculates as [8]:

$$Sh(x) = 2 + \frac{Sh_0 - 2}{F(x)} \tag{23}$$

where $F(x) = (1 + x)^{0.7} \frac{\ln(1+x)}{x}$ and Sh_0 is the Sherwood number calculated from a classical correlation [8]:

$$Sh_0 = 2 + 0.552 \, Re_{ref}^{1/2} \, Sc_{ref}^{1/3} \tag{24}$$

where Re_{ref} and Sc_{ref} are the Reynolds and Schmidt numbers at reference conditions.

4 Model comparison

Among the evaporation rate estimations given by equations (11),(12) and (18), the latter can be assumed to be a more accurate estimation, since it has been obtained without imposing a constant gas density and it was validated

against experimental databases [21]). It is of some interest to notice that for the isothermal case $(T_s = T_\infty)$:

$$\frac{c_\infty}{c_{ref} \int_0^1 \tilde{T}(\zeta)\, d\zeta} = 1$$

and the constant molar density model yields the same results of the variable density one, while the constant mass density model still yields different values. The comparison among the models is made reporting the values of the two ratios: Y^{mol}/Y and Y^{mas}/Y .

To compare the model predictions, different liquids are selected: water, two alcohols, two ketones and seven hydrocarbons, since they may be representative of some applicative fields [28], [29], [30].

All the results presented in the following paragraphs are obtained setting $y_\infty^{(1)} = 0 = \chi_\infty^{(1)}$. Drop temperature was varied from 270K up to the boiling temperature of each liquid at the selected pressure. In case the gas pressure was larger than the critical pressure, the critical temperature was taken as upper limit. The effect of gas temperature and pressure and flow field Reynolds number was also investigated.

Figure 1 shows the values of evaporation rate ratios Y^{mol}/Y and Y^{mas}/Y , for the four families of selected liquids (water, alcohols, ketones and hydrocarbons), versus the vapour molar fraction at drop surface. Equation (4) was used to evaluate the corresponding values of the mass fractions to be used in equation (11). The gas pressure and temperature were fixed equal to 1bar and 600K, respectively, and the drop is assumed to vaporise in stagnant air $(Re = 0)$.

For the water drop test case (Figure 1a), the predictions from the constant mass density model are closer to that of the variable density model, except in a narrow range of operating conditions close to the boiling point.

The difference between the predictions using the two constant density models are much smaller with the two selected alcohols (methanol and ethanol), as shown in Figure 1b. The two models overpredict the values of the evaporation rate compared to the variable density model and the differences reduce as the drop temperature increases. There exists a narrow temperature window where the three models predict almost the same value, then, as the drop temperature approaches the boiling value, the opposite behavior is shown with the two constant density models underpredicting the evaporation rate. Contrary to what was found for the water test case, the evaporation rate predicted by the constant molar density model at low temperature is lower compared to the constant mass density model prediction. This is a direct consequence of the sign of θ, which is negative for water and positive for the

two alcohols. To be noticed that for the methanol test case θ is almost zero ($\theta = 0.108$) and this reflects to the almost negligible differences between the predictions from the two constant density models within the whole range of selected drop temperature since, as above explained, when $\theta = 0$ then $y^{(p)} = \chi^{(p)}$ and $\frac{\rho_{ref}}{c_{ref} M m^{(1)}} = 1$.

Figure 1c shows the test-cases with the two ketones (acetone and 3-pentanone), and more significant differences can be appreciated among the three models. Again the constant mass density model underpredicts the value of the evaporation rate compared to the constant molar density model at low drop temperature and it overpredicts it at higher temperatures, due to the positive value of θ.

Finally, Figure 1d shows the evaporation rate ratio as function of the vapour molar fraction at drop surface using seven hydrocarbons. The results show that the constant molar density model better predicts the evaporation rate for a wider range of operating conditions and the discrepancy against the variable density model increases with molar mass decrease. Since this family of liquids shows the highest differences among the three models, the following analysis on the effect of gas temperature and pressure and Reynolds number was performed selecting n-dodecane as evaporating species.

The effect of gas temperature on the evaporation rate ratios, as function of vapour molar fraction at drop surface for n-dodecane drop vaporising under stagnant air conditions varying the air temperature from 600K up to 2000K (and given air pressure of 1bar) is reported in Figure 2. The discrepancies between the predictions from the two constant density models and the variable density one increase with gas temperature, while the relative difference between the two model predictions is almost independent of gas temperature.

The effect of gas pressure is reported in Figure 3 for the same conditions of Figure 2, setting the gas temperature equal to 2000K. Three values of gas pressure have been selected equal to 1, 10 and 50bar. The results evidence that the increase of the gas pressure reduces the discrepancy between the predictions from both constant density models and those from the variable density model, with the constant molar density model better predicting the evaporation rate for a wider range of operating conditions. To notice that for the test-case with gas pressure equal to 50bar, the two curves stop in correspondence of the value of the drop temperature equal to the critical temperature of n-dodecane.

Finally the effect of convection is shown in Figure 4 for the same operating conditions of Figure 2, fixing the value of gas temperature equal to 2000K and varying the Reynolds number from 0 up to 1000. The graph evidences that as

the Reynolds number increases, the differences among the predictions from the two constant density models reduce at low drop temperature (i.e. low evaporation), while close to the boiling temperature the effect of Reynolds number becomes less important. Furthermore the increase of Reynolds number increases the drop temperature interval where the constant density models underpredict the evaporation rate.

5   Effect of reference temperature

Equations (12) and (18) show that the ratio of the evaporation rate predicted by the constant molar density model and by the variable density one is equal to:

$$\frac{Y^{mol}}{Y} = \frac{\tilde{T}_{ref}}{\int_0^1 \tilde{T}(\zeta)\,d\zeta} \tag{25}$$

where equation (15) was used to eliminate the molar densities. The integral can be written in a more useful form as follows:

$$\int_0^1 \tilde{T}(\zeta)\,d\zeta = \tilde{T}_s A(Y) + [1 - A(Y)] = \tilde{T}_{ref,new} \tag{26}$$

where:

$$A(Y) = \left(\frac{1}{1 - e^{-Y}} - \frac{1}{Y}\right) \tag{27}$$

and it is easy to see that for $Y \simeq 2.15$ the function $A(Y)$ is equal to 2/3 and since $\tilde{T}_{ref} = \frac{2\tilde{T}_s + 1}{3}$ then $\frac{Y^{mol}}{Y} = 1$.

This explains why the predictions of the constant molar density model collapse to that of the variable density one for a given value of the drop temperature, i.e. when $Y = Y^{mol} \simeq 2.15$ (see Figure 2 and 3).

This suggests that the choice of a proper reference temperature, precisely that given by equation (26), renders the performance of the constant molar density model equal to that of the variable density one. Since the coefficient $A(Y)$ depends on the evaporation rate (see Figure 5) this choice cannot be made a priory, but it is interesting to notice that at low evaporating conditions the value of $A(Y)$ equal to 0.5 (the classical 1/2-law) represents a better choice, while at higher evaporating rate conditions (around $Y = 2.15$) the value of $A(Y)$ equal to 2/3, as suggested by the $1/3^{rd}$ law, should be a better choice.

13

6   Conclusions

The effect of using the molar rather then the mass based approach to drop evaporation modelling was analysed. Two drop evaporation models based on the analytical solution of the species conservation equation under the commonly accepted assumption of constant gas density were compared to a recent model that relieves that assumption. The main findings are summarised:

- the two constant density models predict similar values of the evaporation rate for drop conditions far from the boiling point, but the discrepancy increases when drop temperature approaches the boiling condition;

- the constant mass density model agrees better with the variable density model for water drops, while for evaporating species having larger molar mass the discrepancies increase and the constant molar density model performs better.

- both constant density models overpredict the evaporation rate when compared to the variable density model (which is taken as a reference in this study) for temperature well below the boiling temperature and discrepancy increases by larger values of the gas temperature, showing that for evaporation in hot environment (combustion) these models may become less reliable;

- the effect of increasing gas pressure reduces the discrepancy between the predictions from both constant density models and those from the variable density model;

- the increase of the drop Reynolds number under low evaporating conditions reduces the differences among the predictions from the two constant density models and it increases the drop temperature interval where the constant density models underpredict the evaporation rate.

References

[1]   J.C. Maxwell, Diffusion, Encyclopaedia Britannica, ninth ed., vol. 7, 1877, p.214.

[2]   C.T. Crowe, M. Sommerfeld, Y. Tsuji, Multiphase Flows with Droplets and Particles, CRC Press, Boca Raton, 1998.

[3] W. Kays, M. Crawford, B. Weigand, Convective Heat and Mass Transfer, fourth ed., McGraw-Hill, New York, 2005, 1221 Avenue of the Americas.

[4] N.A. Fuchs, Vaporisation and droplet growth in gaseous media, Pergamon Press, London, 1959.

[5] S.S. Sazhin, Advanced models of fuel droplet heating and evaporation, Prog. Energy Combust. Sci. 32 (2006) 162-214.

[6] W.A.Sirignano, Fluid Dynamics and Transport of Droplets and Sprays, 2nd ed., Cambridge University Press, 2010.

[7] S. Sazhin, Droplet and sprays, Springer, 2014.

[8] B. Abramzon, W.A. Sirignano, Droplet vaporization model for spray combustion calculations, Int. Journal of Heat and Mass Transfer 32 (9) (1989) 1605-1618.

[9] C.K. Law, Unsteady droplet combustion with droplet heating, Combust. Flame 26 (1976) 17–22.

[10] C.K. Law, Multicomponent droplet combustion with rapid internal mixing, Combust. Flame 26 (1976) 219–233.

[11] C.K. Law, W.A. Sirignano, Unsteady droplet combustion with droplet heating – II: conduction limit, Combust. Flame 28 (1977) 175–186.

[12] C.K. Law, Internal boiling and superheating in vaporizing multicomponent droplets, AIChE J. 24 (1978) 626–632.

[13] S.S. Sazhin, P.A. Krutitskii, I.G. Gusev, M.R. Heikal, Transient heating of an evaporating droplet, International Journal of Heat and Mass Transfer 53 (13) (2010) 2826-2836.

[14] S.S. Sazhin, P.A. Krutitskii, I.G. Gusev, M.R. Heikal, Transient heating of an evaporating droplet with presumed time evolution of its radius, International Journal of Heat and Mass Transfer 54 (5) (2011) 1278-1288.

[15] R.J. Haywood, R. Nafziger, M. Renksizbulut, Detailed examination of gas and liquid phase transient processes in convective droplet evaporation, J. Heat Transf. 111 (1989) 495–502.

[16] C.M. Megaridis, W.A. Sirignano, Numerical modeling of a vaporizing multicomponent droplet, Int. Symp. Combust. 23 (1990) 1413–1421.

[17] C.H. Chiang, M.S. Raju, W.A. Sirignano, Numerical analysis of convecting, vaporizing fuel droplet with variable properties, Int. J. Heat Mass Transf. 35 (1992) 1307–1324.

[18] J. Schlottke, B. Weigand, Direct numerical simulation of evaporating droplets, Journal of Computational Physics 227 (10) (2008) 5215-5237.

[19] G. Strotos, M. Gavaises, A. Theodorakakos, G. Bergeles, Numerical investigation of the evaporation of two-component droplets, Fuel 90 (4) (2011) 1492-1507.

[20] S. Tonini, G.E. Cossali, An analytical model of liquid drop evaporation in gaseous environment, Int. Journal of Thermal Sciences 57 (2012) 45-53.

[21] S. Tonini, G.E. Cossali, A novel vaporisation model for a single-component drop in high temperature air streams, Int. Journal of thermal Sciences 75 (2014) 194-203.

[22] J.C. Slattery, Momentum, Energy and Mass Transfer in Continua, second ed., vol. 482, R. Krieger Publ., New York, 1981.

[23] S. Tonini, G.E. Cossali, A multi-component drop evaporation model based on analytical solution of Stefan-Maxwell equations 92 (2016) 184-189.

[24] G. Brenn, L.J. Deviprasath, F. Durst, C. Fink, Evaporation of acoustically levitated multi-component liquid droplets, International Journal of Heat and Mass Transfer 50 (2007) 5073–5086.

[25] J. Wilms, Evaporation of Multicomponent Droplets, PhD Thesis, Universität Stuttgart, 2005.

[26] S. Tonini, G.E. Cossali, A novel formulation of multi-component drop evaporation models for spray applications, Int. J. Thermal Sciences 89 (2015) 245-253.

[27] M.C. Yuen, L.W. Chen, On drag of evaporating droplets, Combust. Sci. Tech. 14 (1976) 147-154.

[28] D.R. Sobel, L.J. Spadaccini, Hydrocarbon Fuel Cooling Technologies for Advanced Propulsion, ASME Journal of Engineering for Gas Turbines and Power 119 (1997) 344-351.

[29] Siebers D.L., Liquid-phase fuel penetration in diesel sprays, SAE Paper 980809 (1998).

[30] Z. Luo, S. Som, S.M. Sarathy, M. Plomer, W.J. Pitz, D.E. Longman, T. Lu, Development and validation of an n-dodecane skeletal mechanism for spray combustion applications, Combustion theory and modelling 18 (2) (2014) 187-203.
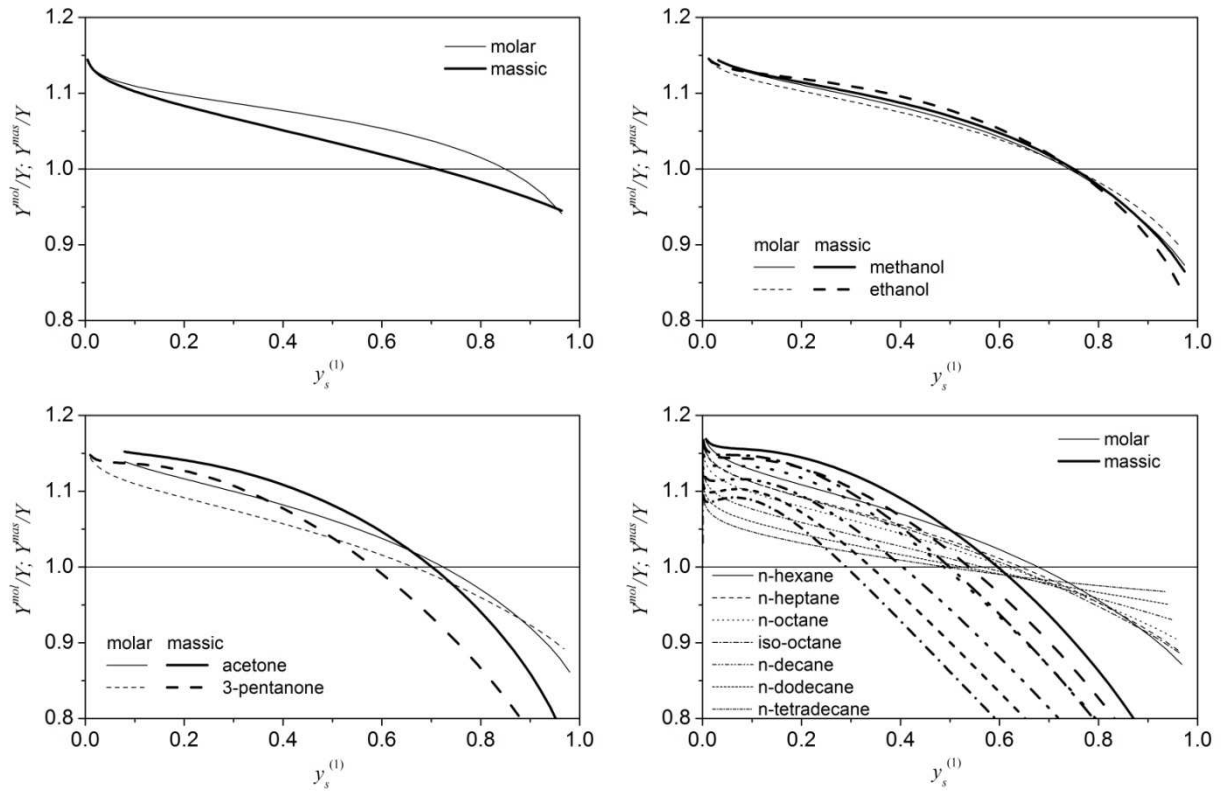
7   Figure captions

Figure 1. Non-dimensional evaporation rate ratio as function of vapour molar fraction at drop surface for (a) water, (b) alcohol, (c) ketone and (d) hydrocarbon drops, at 600K, 1bar and Re=0.
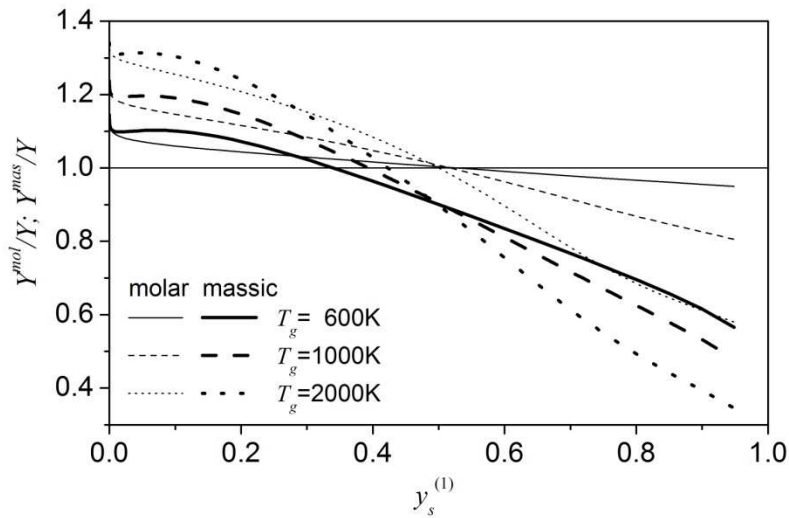
Figure 2. Effect of gas temperature on non-dimensional evaporation rate ratio as function of vapour molar fraction at drop surface for n-dodecane drop at 1bar gas pressure and Re=0.
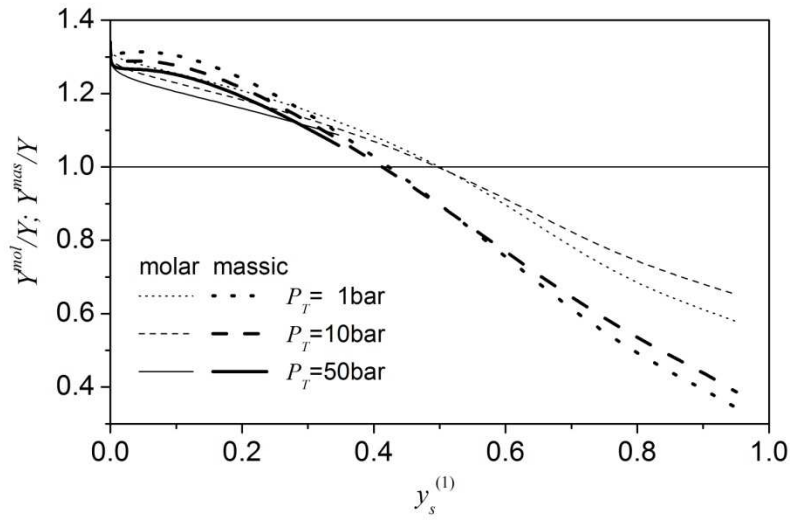
Figure 3. Effect of gas pressure on non-dimensional evaporation rate ratio as function of vapour molar fraction at drop surface for n-dodecane drop at 2000K gas temperature and Re=0.

Figure 4. Effect Reynolds number on non-dimensional evaporation rate ratio as function of vapour molar fraction at drop surface for n-dodecane drop at 2000K gas temperature and 1bar gas pressure.

Figure 5. Value of the coefficient $A(Y)$ in equation 27. The circle corresponds to the case of the '1/3rd' law.

Figure 1. Non-dimensional evaporation rate ratio as function of vapour molar fraction at drop surface for (a) water, (b) alcohol, (c) ketone and (d) hydrocarbon drops, at 600K, 1bar and Re=0.

Figure 2. Effect of gas temperature on non-dimensional evaporation rate ratio as function of vapour molar fraction at drop surface for n-dodecane drop at 1bar gas pressure and Re=0.

Figure 3. Effect of gas pressure on non-dimensional evaporation rate ratio as function of vapour molar fraction at drop surface for n-dodecane drop at 2000K gas temperature and Re=0.
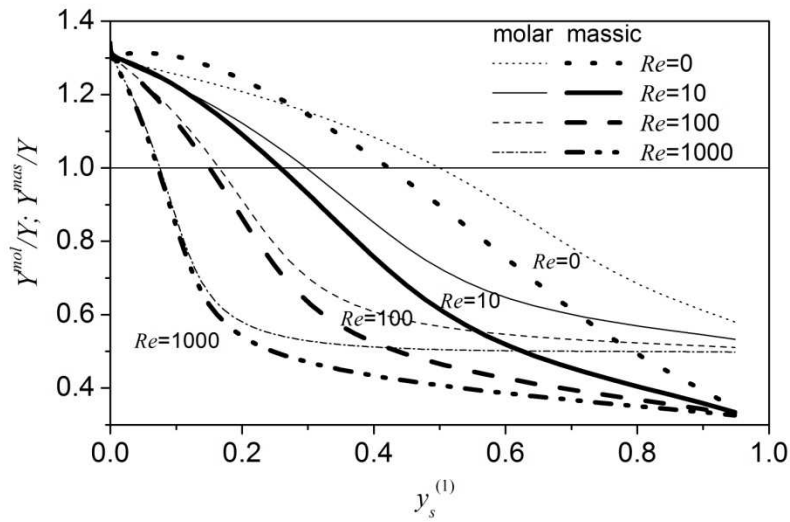

Figure 4. Effect Reynolds number on non-dimensional evaporation rate ratio as function of vapour molar fraction at drop surface for n-dodecane drop at 2000K gas temperature and 1bar gas pressure.
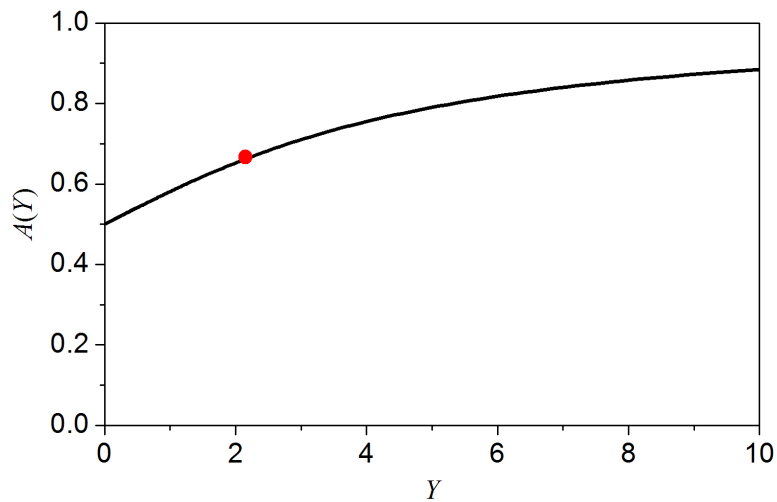

Figure 5. Value of the coefficient $A(Y)$ in equation (27). The circle corresponds to the case of the '1/3rd' law.